Journal of Environmental Chemical Engineering 10 (2022) 108580

Contents lists available at ScienceDirect

Journal of Environmental Chemical Engineering

journal homepage: www.elsevier.com/locate/jece

Sorption of fluorinated greenhouse gases in silica-supported fluorinated ionic liquids

Julio E. Sosa, Rui P.P.L. Ribeiro, Paulo J. Castro, José P.B. Mota, Ana B. Pereiro *, João M. M. Araújo *

LAQV, REQUIMTE, Department of Chemistry, NOVA School of Science and Technology, NOVA University Lisbon, 2829-516 Caparica, Portugal

ARTICLE INFO

Editor: V. Victor

Keywords:
Fluorinated compounds
Refrigerants
Porous solid materials
Solubilization
Separation

ABSTRACT

The Kigali Amendment to the Montreal Protocol limits the global use of fluorinated greenhouse gases (F-gases) and encourages the development of a new generation of refrigerants with lower global warming potential. Therefore, there is a need to develop efficient and sustainable technologies to selectively capture and recycle the F-gases as new environmentally sustainable refrigerants. Here, ionic liquids (ILs) with high F-gas uptake capacity and selectivity were supported on silica and their potential as media for selective F-gas sorption was studied. For this purpose single-component sorption equilibria of difluoromethane (R-32), pentafluoroethane (R-125), and 1,1,1,2-tetrafluoroethane (R-134a) were measured at 303.15 K by gravimetry. The sorption data were successfully correlated using classical models of sorption thermodynamics. The results show that the IL supported in the porous volume and on the external surface of the porous silica controls the F-gas uptake in the composites and that changing the IL's cations and anions allows fine-tuning the selectivity of the sorption process. This work brings crucial knowledge for the development of new materials based on ILs for the selective sorption of F-gases.

1. Introduction

In 1987, the Montreal Protocol determined the phasing-out of second-generation refrigerants based on chlorofluorocarbons, which cause ozone depletion [50]. As consequence, the utilization of man-made fluorinated greenhouse gases (F-gases) based on hydrofluorocarbons (HFCs) has increased drastically for refrigeration and air conditioning applications [11]. These third-generation refrigerants are energetically efficient, non-toxic, have low flammability, and are not harmful to the ozone layer. However, they are potent greenhouse gases (GHGs) with a global warming potential up to 23,000 times greater than that of carbon dioxide and an extensive atmospheric lifetime. While the emissions of all other GHGs in the EU have decreased, the emissions of HFCs have increased by 60% since 1990 [11]. Besides, to accomplish the goals of the United Nations Framework Convention on Climate Change, the Kigali Amendment (entered into force in 2019) regulates the phase-down of HFCs at a global level [12]. In the EU, Regulation Nº 517/2014 imposes restrictions for placing on the market equipment and substances with high GWP.

Because of the commitments to the international agreements and the EU F-gases Regulation, a rapid development of the research on more environment-friendly refrigerant alternatives, including HFCs with lower GWP, hydrofluoroolefins (HFOs), HFC-HFO blends, hydrocarbons, and others natural refrigerant, was observed. Nevertheless, the challenge has been to find alternative refrigerants that ensure a lower GWP and are simultaneously: (i) safe (low flammability and low toxicity); (ii) energy efficient; and (iii) easily recycled and reused. Nowadays, most F-gases recovered from end-of-life equipment are incinerated, contributing to global warming and creating pressure in the refrigeration supply chain. Therefore, there is a clear need to develop technologies to recover and recycle those F-gases from refrigeration and cooling equipment to be recycled into new blends with lower GWP, applying circular economy (an EU priority), avoiding the costs associated with incineration processes, and reducing the GHGs emissions. In most developed countries, and especially in Europe, increasing attention is being paid to the need to separate and recycle the HFCs at the end of life of refrigeration and air conditioning equipment. In fact, in the last years, different projects, such as KET4F-Gas and LIFE-4-Fgases, have been put forward at the European level, aiming at developing technologies to separate HFC blends with high GWP into their pure components.

The capture of pure F-gases and the separation of blends have been extensively investigated using solvents, advanced materials, and

* Corresponding authors.
E-mail addresses: anab@fct.unl.pt (A.B. Pereiro), jmmda@fct.unl.pt (J.M.M. Araújo).

https://doi.org/10.1016/j.jece.2022.108580
Received 30 June 2022; Received in revised form 16 August 2022; Accepted 8 September 2022
Available online 11 September 2022

membrane technology. A variety of studies have dealt with the use of ionic liquids (ILs) and other alternative solvents for the selective uptake of the most commonly used pure F-gases in the EU market (for example, R-134a (1,1,1,2-tetrafluoroethane), R-32 (difluoromethane), and R-125 (pentafluoroethane)) [2,8,9,15–18,23,34,40–44,46,48]. Fluorinated ionic liquids (FILs), defined as ILs containing fluorinated alkyl chains with at least four carbon atoms, form polar, nonpolar, and fluorinated domains with the ability to solubilize and interact simultaneously with three totally different moieties [30–32]. Moreover, FILs are highly tunable, with a vast range of possible variations in the size of the three different domains, which allows different types of interactions. Additionally, FILs containing short perfluorinated or hydrogenated alkyl chains are not toxic for different human cell lines and aquatic species [30,51,52]. Finally, the fluorination of ILs is a key process to decrease the viscosity and therefore to increase mass transfer [30,38]. Previous work has shown that ILs have high F-gas absorption capacity and that the properties of the absorbed F-gas play a key role in its effective absorption [46]. Moreover, the combination of FILs and membrane technology has been demonstrated to be relevant for the separation of refrigerants mixtures, as addressed by Pardo et al. [26–29] and Hermida-Merino et al. [13].

The adsorption of pure F-gases has also been studied on various adsorbent types [55], such as silica and activated carbons [1,4,5,7,19,20,36,37,47], zeolites [39,53], and metal-organic frameworks (MOFs) [24,54]. The investigation of porous materials for separation processes has advanced greatly in the last decades, as the selection of materials with different properties, such as surface area and pore volume and dimensions, and functionalization allows to direct the selectivity toward a specific species of a gas blend, allowing to separate it from the other components of the mixture.

The support of ILs in solid porous materials represents an advantage to increase the contact area between the gaseous sorbate and the solubilization media, increasing the mass transfer. Some authors have already studied the preparation of mesoporous silica with impregnated ILs for CO_2 sorption [14,21,35], CO_2 conversion [49], and desalination [6]. In this work, we are stepping forward in the study of FILs and other fluoro-containing ILs (with a variety of functional groups and sizes of the perfluorinated chain) supported in silica, aiming at increasing the contact area to increase the sorption capacity. While a variety of new materials, such as MOFs, have been developed in the last years for the adsorption of F-gases with very high adsorption capacity [54], these materials are still difficult to produce in high amounts and have high costs. Therefore, in this study, we have selected silica, a cheap, well-studied and widely available porous material for the support of ILs.

We report the measurement and comparison of the sorption properties of R-32, R-125 and R-134a on silica and nine different silica/IL composites at room temperature. The experimental data are successfully correlated with the Sips adsorption isotherm model and an analogy model with the adsorption potential theory (APT). Since various fluorinated refrigerants composed of different F-gases are used industrially, the study of the selective separation of different F-gases from mixtures is crucial. To this end, we predict the sorption equilibria of two commercial refrigerants, R-410A (a binary blend of R-32 and R-125) and R-407 F (a ternary blend of R-32, R-125, and R-134a), in the studied composites, assuming the IL/F-gas system in the silica/IL composites behaves as an ideal mixture. Moreover, the selectivity is evaluated at different equilibrium pressures. This work presents a step forward in the study of single- and multi-component F-gas sorption in ILs supported on porous materials and in the still poorly explored area of F-gas capture and separation from commercial refrigerants.

2. Characterization of the composites

Each composite was prepared by mixing 40 wt% IL with 60 wt% fumed silica according to the experimental procedure detailed in the SI. Given that the specific volumes of the tested ILs are in the range 0.65–0.91 cm^3/g, 40-wt% IL is 30–85% in excess of the amount required to completely fill the $0.33 \times 0.6 = 0.20$ cm^3/g porous volume of the composite with bulk liquid IL. The composites were characterized in terms of BET surface area (S_{BET}) and pore volume (V_p) (SI shows the experimental procedure). The surface area and porous volume of silica are significantly decreased when it is impregnated with 40-wt% IL (see Table S2 of SI). The S_{BET} and V_p values decreased between ~60% for the $SiO_2/[C_2C_1Im][C_8F_{17}SO_3]$ composite and ~80% (S_{BET}) and ~90% (V_p) for $SiO_2/[C_2C_1Im][C_1CO_2]$. These results indicate that the IL not only penetrated into the pore volume of the silica but also covered the external surface of the silica particles, rather than existing as droplets surrounded by a silica envelope, as observed in other studies [35].

The morphology of the composites was evaluated and compared with those of pure IL and fumed silica by scanning electron microscopy (SEM) (SI shows the experimental procedure). Figs. S4–S6 of SI compare the SEM images of: (i) fumed silica; (ii) three pure ILs, ($[C_2C_1Im][C_1CO_2]$ as reference IL, $[C_2C_1Im][N(CF_3SO_2)_2]$, and $[C_2C_1Im][C_4F_9SO_3]$); and (iii) the composites prepared with these ILs. The morphology of the composites is very similar to that of pure silica and has notable differences from that of pure ILs. Moreover, the energy-dispersive X-ray spectroscopy (EDS) analysis of each sample (see Figs. S4–S6 of SI) detected fluorine atoms on the surface of the composites prepared with ILs containing fluorine atoms but not on the silica samples. These results indicate that some of the ILs are located on the external surface of the silica particles and the rest inside of their porous volume, reinforcing the previous conclusions from ASAP results.

3. Results and discussion

3.1. Gas sorption in the silica/IL composites

The procedure for determining the F-gas sorption on the composites is detailed in the SI. The equilibration time required for measuring each experimental data point was about 40 min. Sorption data of each F-gas on silica and the composites are presented as excess sorption, q_{ex}, in Fig. 1 and total sorption, q, in Fig. S7 of SI, as a function of equilibrium gas pressure (see also Table S4 of SI). The sorption and desorption branches of the isotherm are superimposable, indicating the inexistence of hysteresis between the sorption and desorption processes (see Fig. S8 of SI). Fig. 1 shows that for gas pressures below ca. 0.18 MPa the porous silica adsorbs more F-gas than the pure ILs and the composites; however, above $P = 0.18$ MPa, the F-gas uptake by the pure ILs is higher than by the porous silica and the composites.

Since to predict binary adsorption and calculate selectivities it is necessary to manipulate analytical expressions of loading as a function of pressure, the sorption data were fitted by a Sips isotherm model [45], as detailed in the SI, with good agreement between calculated and experimental data. The Sips parameters determined for each composite/F-gas pair are listed in Table S5 of SI and the fittings are illustrated in Fig. S7 of SI as dashed lines. Although the Sips model was originally developed as a combined form of Langmuir and Freundlich models for predicting the adsorption in heterogeneous systems and circumventing the limitation of the rising adsorbate concentration associated with the Freundlich isotherm, we use it here as a general three-parameter model with enough flexibility to adequately fit our experimental sorption data.

The purpose of supporting the ILs on silica, a material with a relatively high porous volume, is to enhance the mass transfer and increase the contact area with the F-gas. The sorption capacity and selectivity of the prepared composites towards R-32, R-125, and R-134a were evaluated. Due to the high tuneability of the ILs, the appropriate combination of cation and anion allows the sorption and selectivity of a given gas to be optimized. The absorption of R-32, R-125, and R-134a into different ILs containing fluorine atoms was previously studied [46]. Here, six different ILs based on two cations ($[C_2C_1Im]^+$ and $[C_2C_1py]^+$) and on five different anions ($[C_1CO_2]^-$, $[CF_3SO_3]^-$, $[N(CF_3SO_2)_2]^-$, $[C_4F_9SO_3]^-$,

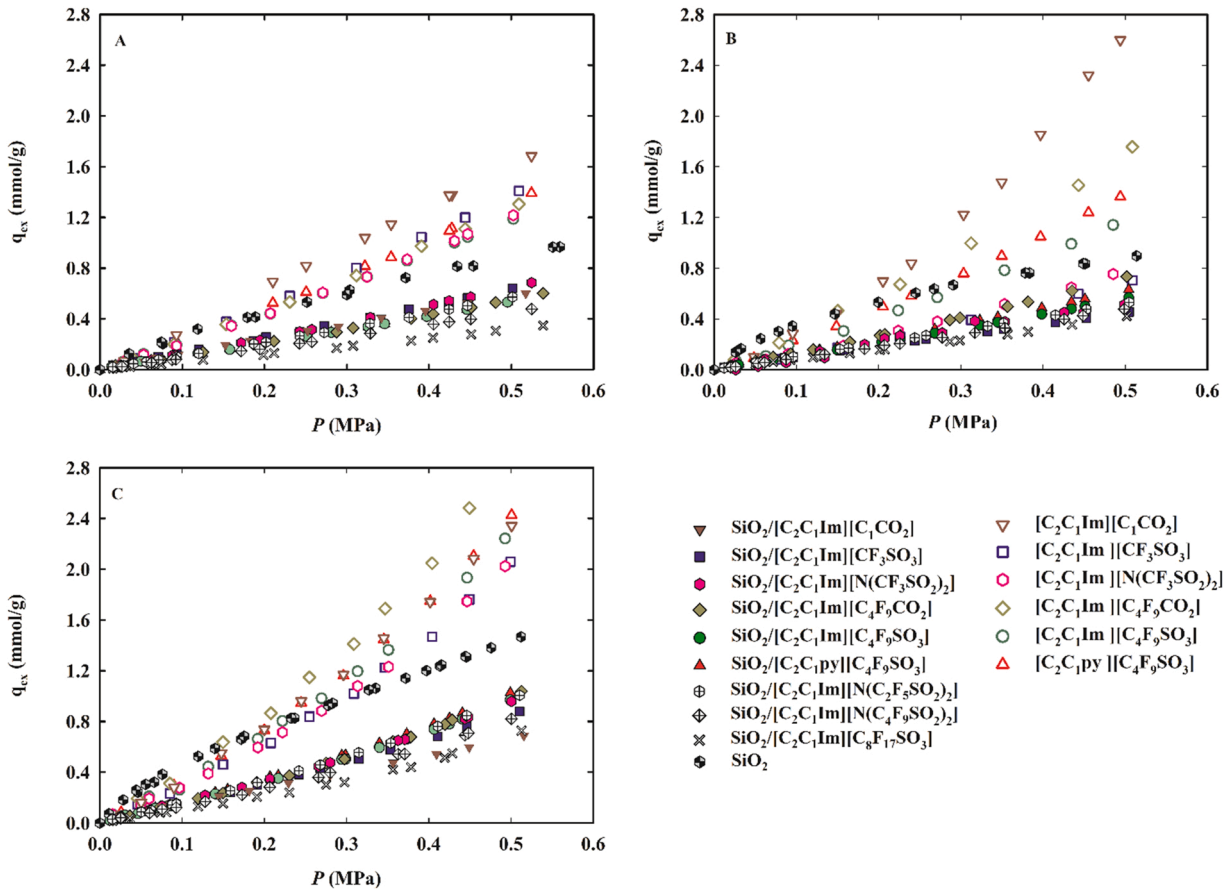

Fig. 1. Sorption equilibrium isotherms, at 303.15 K, of R-32 (panel A), R-125 (panel B), and R-134a (panel C) on the fumed silica, composites studied in this work, and on pure ILs studied previously [46].

$[C_4F_9CO_2]^-$) were examined [46]. Additionally, three other ILs, $[C_2C_1Im][N(C_2F_5SO_2)_2]^-$, $[C_2C_1Im][C_8F_{17}SO_3]^-$, and $[C_2C_1Im][N(C_4F_9SO_2)_2]^-$, are supported on silica to prepare composites used to study the effect of increasing the size of the perfluorinated chain of the IL anion on gas sorption and selectivity.

Fig. 1 compares our experimental results with previously published absorption data of pure ILs [46] over the entire pressure range studied in this work. F-gas absorption in pure IL shows improved performance relative to the SiO_2/IL composite and fumed silica. However, when a correction factor of 0.4 is applied to the IL sorption data on the composite (to account for 40% weight of IL in the composite), the uptake values for both pure IL and its composite are similar, in most cases with slightly better results for the composite (Fig. S9 of SI), due to the effect of the force field exerted by the internal surface of the silica on the confined IL which improves its absorption capacity. These results show that F-gas sorption in the composites is controlled by the IL. Moreover, F-gas solubility in the pure ILs is higher than the F-gas sorption in the porous silica.

As noted earlier for pure ILs [46], the use of ILs with different cations and anions, and especially with different numbers of fluorine atoms in the anion, strongly influences the solubility and selectivity of the gas. In this work, it was observed that the ILs play a major role in F-gas sorption in the composites. Moreover, the preparation of composites using different ILs led to significant differences in F-gas sorption, with trends similar to the ones observed for gas solubility in pure ILs (see Fig. 1 and Fig. S7 of SI). All composites have a higher sorption capacity to R-134a than to the other two F-gases (see Fig. S10 of SI).

The presence of a carboxylate group, instead of a sulfonyl group, in the IL anion slightly enhances the sorption of R-125 but not of R-32 and R-134a (see Fig. S11 of SI). The same tendency is observed for the pure ILs studied in the work of [46] (Fig. 1). Interestingly, R-125 has also good solubility in the pure $[C_2C_1Im][C_1CO_2]$, suggesting that polar interactions with the carboxylate group may play an important role in the solubility of R-125 [46]. Similar conclusions were obtained by Asensio-Delgado et al. [3], where the sorption of R-125 in carboxylate-based ILs was observed to deviate from the Regular Solution Theory [3].

While the presence of either an imidazolium or a pyridinium group in the IL cation does not significantly affect F-gas sorption (see Fig. S12 of SI), the size of the perfluorinated chain plays a key role in the sorption capacity of the studied ILs (see Figs. S13 and S14 of SI). The increment from $[CF_3SO_3]^-$ to $[C_4F_9SO_3]^-$ has no significant effect on F-gas sorption but the composites prepared from ILs with the highest number of carbons in the perfluorinated chain ($[C_2C_1Im][C_8F_{17}SO_3]$ and $[C_2C_1Im][N(C_4F_9SO_2)_2]$) have the poorest sorption capacity for the three F-gases. However, the influence of the increment of the fluorinated alkyl chain length is higher for the sorption of R-32 and R-134a than for the adsorption of R-125, demonstrating specific interactions with this F-gas.

On the other hand, the composites containing the two studied conventional fluoro-containing ILs ($[C_2C_1Im][CF_3SO_3]$ and $[C_2C_1Im][N(CF_3SO_2)_2]$) presented the best sorption capacities for R-32. On the other hand, composites containing ILs with up to 4 carbons in the perfluorinated chain present the best results for R-134a and R-125 (see Figs. S13 and S14 of SI). The presence of ramified perfluorinated chains in the anion of the ILs does not significantly affect the uptake of R-125 and R-134a (see Fig. S14 of SI). However, the increase in the anion size and the change of linear to ramified chains in the ILs anion leads to a decrease in gas uptake in the case of R-32 (see Fig. S14 of SI).

These effects in gas uptake are in accordance with those previously observed for pure ILs [46], revealing that the properties of the ILs are

commanding the sorption of the F-gases in the composites. In this way, the sorption of the F-gases containing a higher number of fluorine atoms (R-125 and R-134a) is enhanced in composites prepared with FILs (fluorinated ILs with fluorinated chain lengths equal to or greater than 4 carbon atoms), relatively to conventional fluoro-containing ILs (with perfluorinated chains shorter than 4 carbon atoms). These results highlight the key role of the fluorinated alkyl side chain (fluorinated nanosegregated domain) of the IL, either pure or as a composite, in the solubility of the studied F-gases.

The sorption of each F-gas was also evaluated based on the Henry's law constant, H_i, [33] defined as

$$H_i\left(T,P\right) = \lim_{x_i \to 0} \frac{f_i^L}{q_i} \tag{1}$$

where f_i^L is the fugacity of gas i and q_i the uptake of gas by the sorption medium expressed as total or excess sorption (mmol/g), under infinite dilution conditions ($\lim_{f_i \to 0} q_i = \lim_{f_i \to 0} q_i^{ex}$). Since under thermodynamic equilibrium the fugacity of the F-gas in the sorbent phase is equal to the fugacity in the gas phase, the Henry's law [33] can be rewritten as follows:

$$H_i(T) = \lim_{P_i \to 0} \frac{P_i}{q_i} \tag{2}$$

where P_i is the partial pressure of F-gas in the gas phase. Therefore, the Henry constant is the proportionality value between the partial pressure of F-gas in the gas phase and its solubility in the sorbent phase, under infinitely dilute conditions. The slope of the tangent at $P = 0$ of the experimental (q, P) data is the Henry's law constant and consequently, a smaller value of this parameter corresponds to a higher gas solubility.

The comparison with the pure ILs [46] was also made through the Henry's law constants (see Fig. 2 and Table S6 of the SI), which confirmed that gas sorption into the composites is lower than into the pure ILs. Moreover, these results clearly show that the tendencies of gas sorption in the composites are identical to those in pure ILs. Finally, it is observed that under infinite dilution (low pressure) conditions, silica has the best gas adsorption capacity, contrary to what is observed at higher pressures, where the pure ILs have higher absorption capacity (see Fig. 1).

3.2. An analogy with the adsorption potential theory (APT)

A formulation similar to the Adsorption Potential Theory (APT) was applied to the sorption equilibrium data in the composites and silica, as detailed in the SI. As in the APT [10], the sorbed amount of gas, q, measured as an equivalent volume of condensed gas, W, is expressed as

$$W = qV_m = W(\Phi) \tag{3}$$

where V_m is the molar volume of the gas if it were condensed into a liquid phase,

$$\Phi = RT\ln(f_s/f) \tag{4}$$

is usually referred to as the sorption potential [10], R is the ideal gas constant, T the system temperature, f the fugacity, and f_s the saturation fugacity (to account for non-ideal gas behavior at high pressure). However, we prefer to identify Φ as the difference in free energy (or chemical potential) when a gas molecule is moved from the gas phase to its condensed state. Since in this work the sorption data were measured at a single temperature, the formulation above is perfectly valid because Eqs. (3) and (4) are equivalent to simply stating that $q = q(P)_{\text{fixed } T}$.

But, inspired by the APT, one can go a step further and test whether introducing an affinity coefficient β, as a scaling factor of Φ, collapses the curves $W_i(\Phi_i)$ of the different gases in the same composite into a single characteristic curve $W(\Phi_i/\beta_i)$ [10] Thus, Eq. (3) is replaced by

$$W_i = q_i V_{i,m} = W(\widetilde{\Phi}_i), \quad \widetilde{\Phi}_i = \frac{\Phi_i}{\beta_i} \tag{5}$$

where $\widetilde{\Phi}_i$ is the sorption potential scaled by β_i. In the literature, β is often correlated to the molecular parachor of the adsorbate.

Table S3 of SI lists the values of β that collapse the curves $W_i(\widetilde{\Phi}_i)$ of the three different F-gases in the same composite into a single characteristic curve. For reference, we also include the values obtained for silica and those given by a correlation often used for adsorption in carbon materials (see SI). These characteristic curves are plotted in Fig. 3 and fitted to an equation similar to the Dubinin–Astakhov (D–A) model. The D–A isotherm parameters obtained from the curve fitting are indicated in Table S7 of SI and the comparison between the experimental sorption isotherms and the D–A model fitting is presented in Fig. S15 of SI.

Somewhat surprisingly, not only is it possible to collapse the sorption data of the three F-gases on the same composite into a single charac-

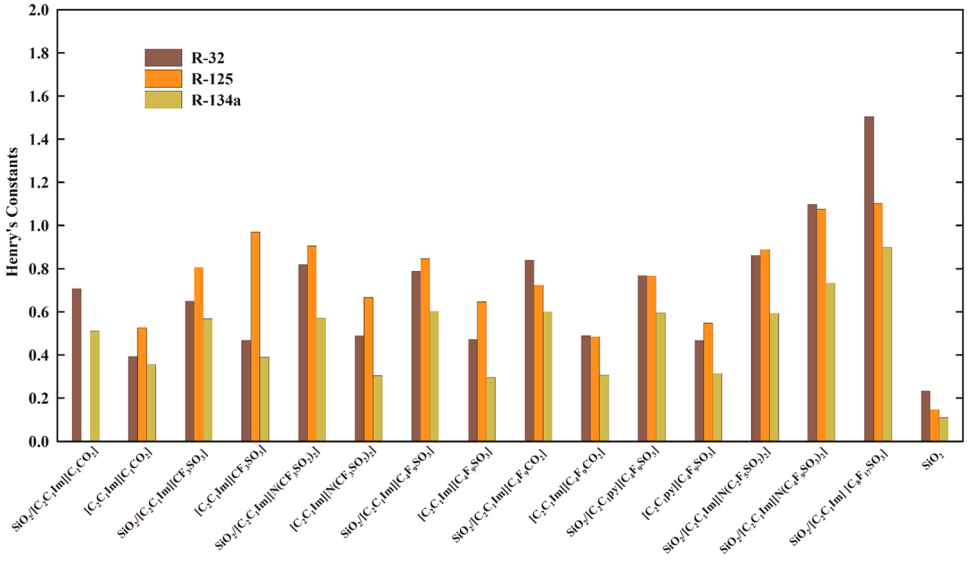

Fig. 2. Henry's Law constants (in MPa g mmol^{-1}) determined for the sorption of R-32, R-125, and R-134a, at 303.15 K, in the SiO_2/ILs composites studied in this work and pure ILs studied previously [46].

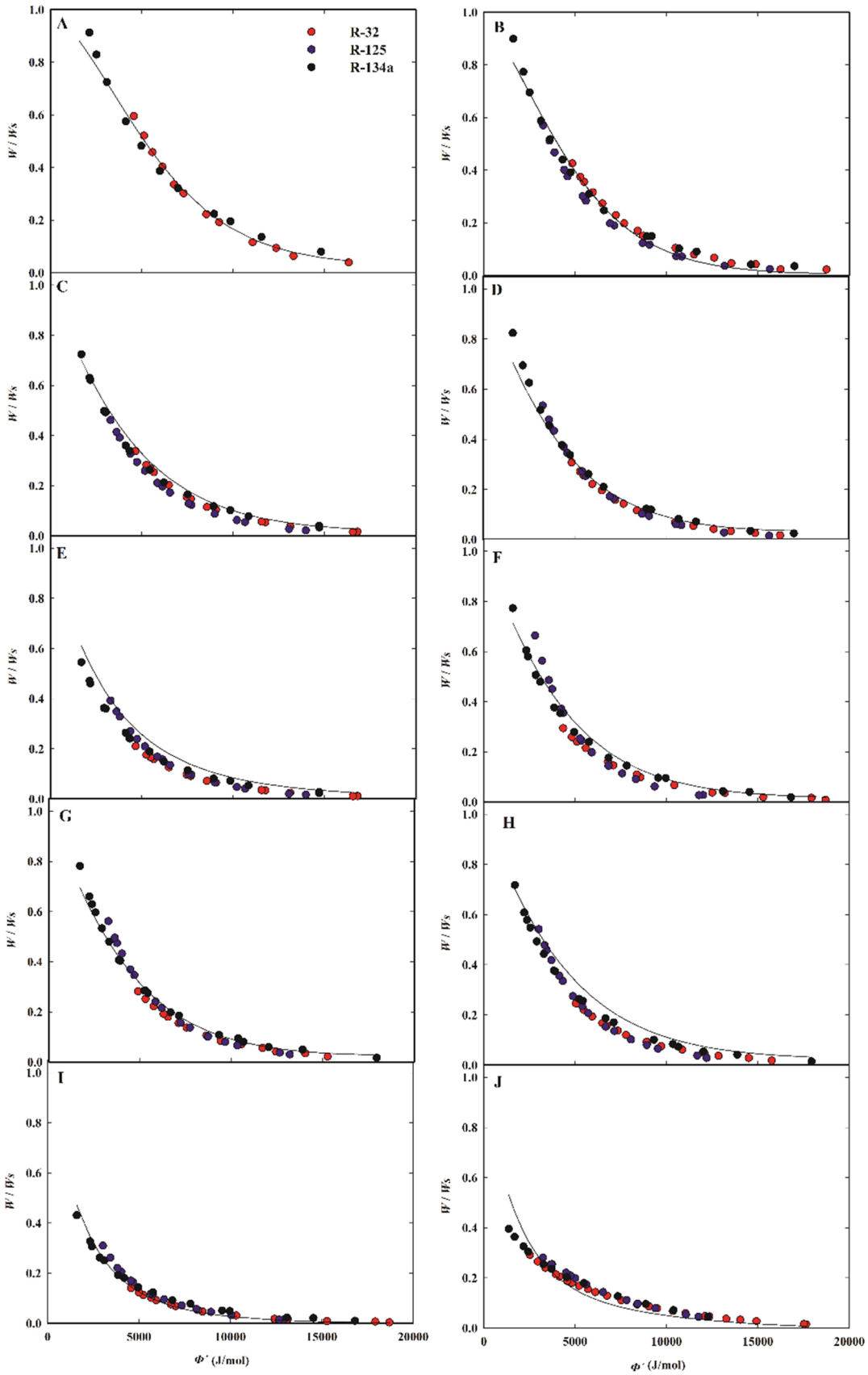

Fig. 3. Characteristic curves obtained by adsorption potential theory (APT) using the experimental sorption data of R-32, R-125, and R-134a at 303.15 K on SiO_2/$[C_2C_1Im][C_1CO_2]$ (panel A), SiO_2/$[C_2C_1Im][CF_3SO_3]$ (panel B), SiO_2/$[C_2C_1Im][N(CF_3SO_2)_2]$ (panel C), SiO_2/$[C_2C_1Im][N(C_2F_5SO_2)_2]$ (panel D), SiO_2/$[C_2C_1Im][N(C_4F_9SO_2)_2]$ (panel E), SiO_2/$[C_2C_1Im][C_4F_9CO_2]$ (panel F), SiO_2/$[C_2C_1Im]$ $[C_4F_9SO_3]$ (panel G), SiO_2/$[C_2C_1py]$ $[C_4F_9SO_3]$ (panel H), SiO_2/$[C_2C_1Im][C_8F_{17}SO_3]$ (panel I), and SiO_2 (panel J). Dashed lines represent the data fitted to the Dubinin–Astakhov (D–A) equation.

teristic curve by using an affinity coefficient but also the obtained values of β are almost independent of the type of composite but different from those for pure silica. These results are another indication that the IL supported in the porous volume and on the external surface of the porous silica controls the F-gas uptake in the composites.

3.3. Prediction of multicomponent sorption using the ideal adsorption solution theory (IAST)

In this work, the sorption equilibria of R-410A (R-32/R-125, 50/50 wt%), R-407 F (R-32/R-125/R-134a, 30/30/40 wt%), and of each component of these systems, were predicted using the Ideal Adsorption Solution Theory (IAST) [25]. These predictions were based on the experimentally determined isotherms of the pure F-gases R-32, R-125, and R-134a, fitted with the Sips model. The study was applied to all composites over the pressure range 0.01–0.6 MPa (Tables S8 and S9 of SI and Fig. S16 of SI). The equilibrium mole fractions of the gas phase (y) are those of the commercial F-gases blends: $y^0_{R\text{-}32} = 0.70$ and $y^0_{R\text{-}125} = 0.30$ for R-410A, and $y^0_{R\text{-}32} = 0.47$, $y^0_{R\text{-}125} = 0.21$, and $y^0_{R\text{-}134a} = 0.32$ for R-407 F. The uptake of both gas mixtures increases with increasing pressure. Silica and the composites prepared with FILs with up to ten fluorine atoms in the anion have the highest R-410A and R-407 F sorption capacities, while the composites prepared from fluoro-containing ILs (with fluorinated chains shorter than 4 carbon atoms) and FILs with 17 or 18 fluorine atoms in the anion have the lowest sorption capacities at the highest pressures.

3.4. Selectivity for the separation of F-gases from commercial refrigerants

The capacity of the composites studied in this work for the separation of R-410A and R-407 F refrigerants in their components (R-32, R-125, and R-134a) was analyzed using the predictions determined by IAST. The gas selectivity (S) at 303.15 K of each composite and silica for the separation of a gas i from the mixture with a gas j was determined as follows [22]:

$$S_{ij} = \frac{x_i/x_j}{y_i/y_j} \tag{6}$$

where x_i and x_j are the sorbed molar fractions of gas i and of gas j, respectively, and y_i and y_j are the molar fractions of gas i and of gas j in the gas phase at equilibrium, respectively.

The capacity of each composite and silica for the separation of the commercial refrigerant R-410A into its components (R-32 and R-125) was evaluated by determining the R-32/R-125 selectivity, using the IAST results. If the selectivity values are greater than 1, R-32 is preferentially sorbed, and if these values are less than 1, R-125 is preferentially sorbed. The value of the selectivity was determined as a function of pressure for the equilibrium gas-phase composition corresponding to that of bulk R-410A and the results are plotted in Fig. 4 (see values in Table S10 of SI). At low pressures, most composites are selective towards R-32 (with $SiO_2/[C_2C_1Im][C_4F_9SO_3]$ presenting the highest selectivity), while silica, $SiO_2/[C_2C_1Im]$ $[C_4F_9CO_2]$, and $SiO_2/[C_2C_1Im][C_8F_{17}SO_3]$ are selective towards R-125. At higher pressures, the R-32/R-125 selectivity is higher for $SiO_2/[C_2C_1Im][CF_3SO_3]$ and $SiO_2/[C_2C_1Im][N(CF_3SO_3)_2]$, and the R-125/R-32 selectivity is higher for $SiO_2/[C_2C_1Im][C_4F_9CO_2]$, $SiO_2/[C_2C_1py][C_4F_9SO_3]$, and $SiO_2/[C_2C_1Im][C_8F_{17}SO_3]$. In this same pressures range, the selectivity of silica approaches 1 and the selectivity of $SiO_2/[C_2C_1py][C_4F_9SO_3]$ is shifted towards R-125.

In the case of the R-407 F blend, a ternary mixture of R-32, R-125, and R-134a, the selectivities for the separations of R-32/R-125, R-134a/R-32, and R-134a/R-125 were determined as a function of pressure at 303.15 K for the equilibrium gas-phase composition of the bulk R-407 F. The results are shown in Fig. 5, and Table S11 of SI. All composites are selective for the separation of R-134a from their mixtures with the other two gases (panels B and C of Fig. 5), with silica presenting the highest selectivities. Higher R-32/R-125 selectivities were obtained for the composites prepared with the conventional fluoro-containing ILs ($SiO_2/[C_2C_1Im][CF_3SO_3]$ and $SiO_2/[C_2C_1Im][N(CF_3SO_3)_2]$) at all range of pressures and to the composite prepared with $SiO_2/[C_2C_1Im][C_4F_9SO_3]$ at low pressures. Higher R-125/R-32 selectivities were obtained for silica and for the composite prepared from $SiO_2/[C_2C_1Im][C_8F_{17}SO_3]$ at low pressures, and for the composites prepared from $SiO_2/[C_2C_1Im][C_8F_{17}SO_3]$, $SiO_2/[C_2C_1py][C_4F_9SO_3]$, and $SiO_2/[C_2C_1Im][C_4F_9CO_2]$ at higher pressures.

In order to determine if the support of ILs into fumed silica has effects on the gas selectivity, the ideal selectivity for each binary pair of gases i and j was also determined using the Henry's constants of each gas i and j (H_i and H_j) in the same sorbent as follows [22]:

$$S_{ij} = \frac{H_j}{H_i} \tag{7}$$

The comparison of the ideal selectivities of fumed silica, composites, and pure ILs is represented in Fig. S17 of SI and the values are also presented in Table S12 of SI. The results clearly show that, when compared to the composites, the pure ILs have a greater capacity to separate these F-gas mixtures, with the best performance being achieved for the separation of the R-134a + R-125 mixture. Pure fumed silica has the highest capacity for the separation of the R-134a + R-32 mixture. The results show that the selectivities of the composites and ILs follow

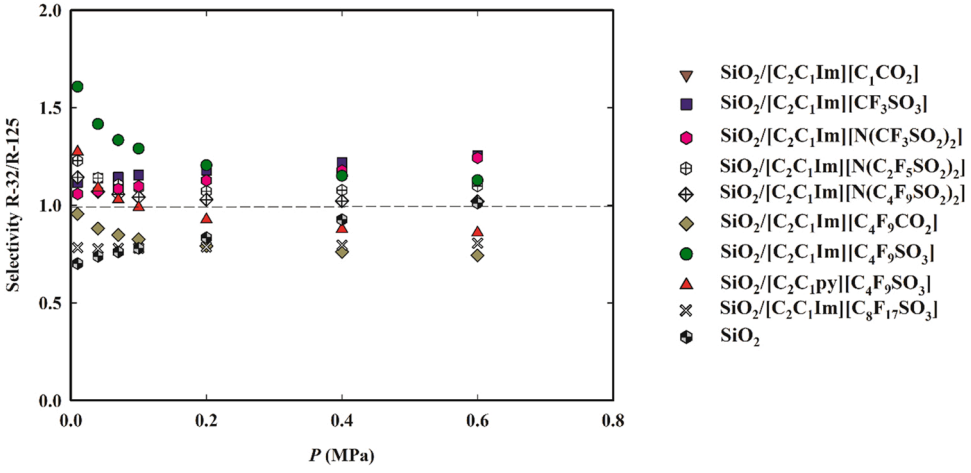

Fig. 4. Selectivity of SiO_2 and the SiO_2/composites to the separation of the mixture R-32 / R-125 as a function of pressure at 303.15 K from the commercial R-410A refrigerant ($y_{R\text{-}32} = 0.7$ and $y_{R\text{-}125} = 0.3$).

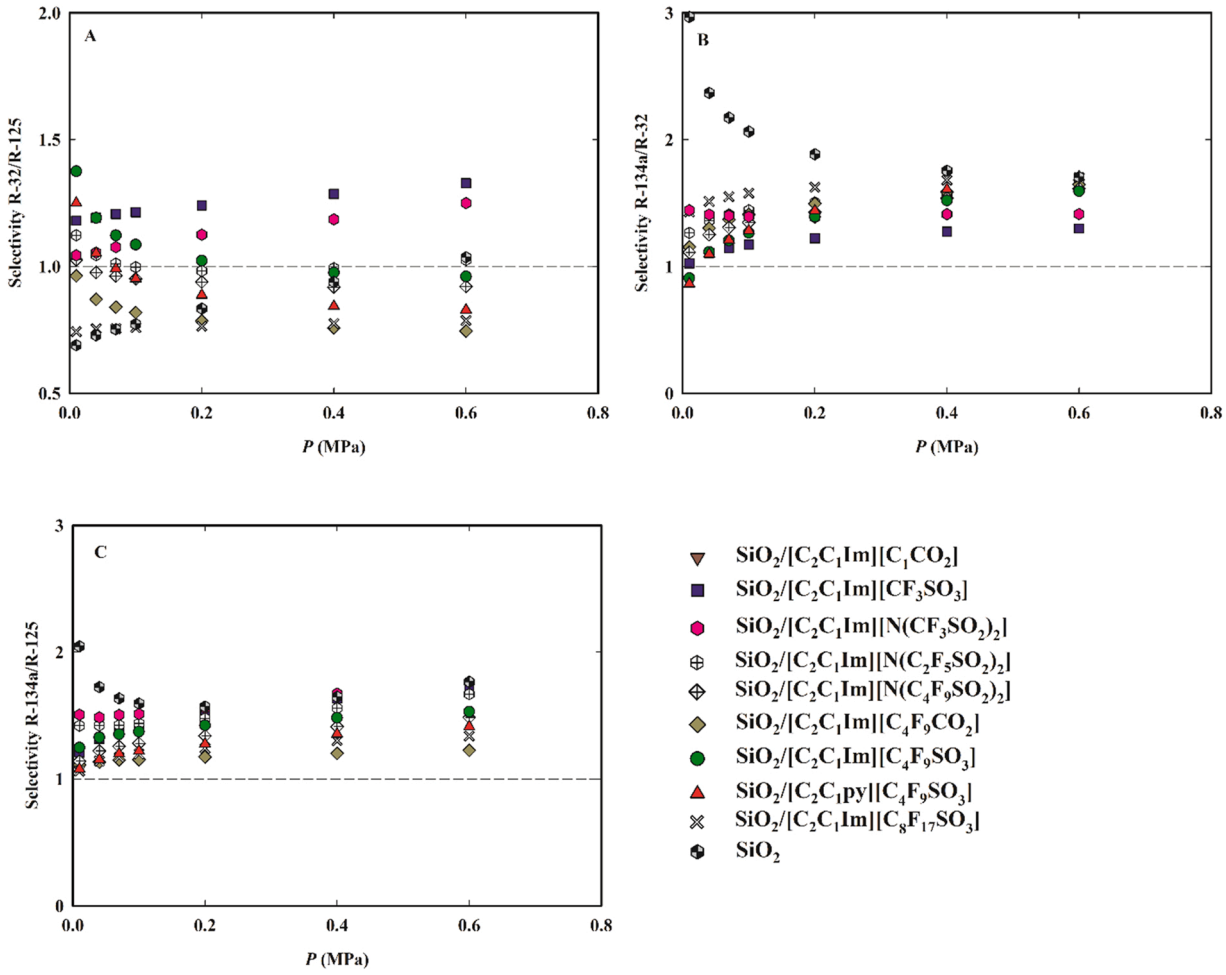

Fig. 5. Selectivity of SiO_2 and the SiO_2/composites to the separations of: R-32/R-125 (panel A); R-134a/R-32 (panel B); and R-134a/R-125 (panel C), as a function of pressure at 303.15 K from the commercial refrigerant R-407 F ($y_{R\text{-}32} = 0.47$, $y_{R\text{-}125} = 0.21$, and $y_{R\text{-}134a} = 0.32$).

the same trends, with composites presenting similar or lower values in most cases. The exceptions are $SiO_2/[C_2C_1Im][C_4F_9CO_2]$, which is more selective towards R-125 over R-32, and $SiO_2/[C_2C_1Im][C_1CO_2]$, which is more selective towards R-134a over R-32. All composites are selective towards R-134a over R-32 and R-125. As reported before for pure ILs, an increase in the number of fluorine atoms favors the selectivity for the separation of the two F-gases with the most different sizes, R-134a and R-32. The composite with the highest selectivity for the R-134/R-32 separation is $SiO_2/[C_2C_1Im][C_8F_{17}SO_3]$. The results presented here also show that an increase in the number of fluorine atoms moves the selectivity towards R-125 for the R-32 + R-125 mixture. The same behavior is observed when the functional group in the IL anion is changed from a sulfonyl to a carboxylate group. $SiO_2/[C_2C_1Im][CF_3SO_3]$ presents the highest selectivity towards R-32 over R-125 while $SiO_2/[C_2C_1Im][C_8F_{17}SO_3]$ and fumed silica present the best selectivity toward R-125 over R-32. Moreover, the separation of mixtures of R-134a and R-125, which have similar sizes, is favored in composites prepared with ILs with ramified perfluorinated chains in the anion.

4. Conclusions

Fluorinated ionic liquids have optimal properties for the selective absorption of F-gases. In this work, we supported different FILs and other fluoro-containing ILs in silica with the aim to increase the contact area and mass transfer between the F-gas and the ILs. The results from BET superficial area, pore volume analysis, SEM, and EDS suggest that the ILs are located at the surface and inside the pores of silica. These composites and pure fumed silica were evaluated for their capacity to sorb the three most used pure F-gases used in refrigeration and air conditioning equipment (R-32, R-125, and R-134) at 303.15 K and pressures up to 0.54 MPa. The sorption data were successfully correlated with the Sips equation and by an analogy to the Adsorption Potential Theory. The sorption data of these three gases in each composite were successfully collapsed into a single characteristic curve, which was well fitted by the Dubinin–Astakhov (D–A) model.

The capacity of the composites and silica to sorb the three F-gases was compared to the previously published results for the pure ILs [46]. Moreover, the Henry's Law constants were also calculated to obtain valuable information on gas solubility at diluted conditions. At high pressures, the pure ILs present higher gas solubility capacity than silica, evidencing the advantages of using ILs for F-gases sorption. From these comparisons, it became clear that similar effects on gas solubilization occur when the same modifications were performed in the cation or anion of the pure IL or the corresponding composites. Therefore, it is evident that the properties of the ILs are commanding the sorption of the F-gases.

Using the Ideal Adsorption Solution Theory (IAST), the sorption of two commercial refrigerants, R-410A and R-407 F, in each composite and silica was calculated at different pressures. Then, the selectivity of the composites and silica to each component of the F-gas blends was determined. The results show that the composites are selective towards R-134a in relation to either R-32 or R-125. Moreover, better separations are obtained for the R-407 F refrigerant than for the R-410A blend. Pure ILs presented higher R-134a/R-125 selectivities, compared to fumed

silica, which confirms that ILs are advantageous systems for the separation of R-134a and R-125.

The results presented in this work show that ILs have good sorption capacities for the selective separation of F-gas from gas blends and that ILs present in the composites control not only gas solubility but also gas selectivity. By supporting the ILs into a porous material, it was possible to obtain a new material, maintaining the selective sorption capacities of the ILs. Thus, this work obtains key information to the fundamental understanding of the behavior of these alternative materials and opens the road for the development and manipulation of new materials based on ILs for the selective uptake of F-gases.

Author contributions

The manuscript was designed and written with the contributions of all authors. All authors have approved the final version of the manuscript.

Funding

This work was financed by national funds from FCT/MCTES (Portugal) through Associate Laboratory for Green Chemistry–LAQV (UIDB/50006/2020 | UIDP/50006/2020), the contracts of Individual Call to Scientific Employment Stimulus 2020.00835.CEECIND (J.M.M. A.) / 2021.01432.CEECIND (A.B.P.), the Norma Transitória DL 57/2016 Program Contract (R.P.P.L.R.), and the project PTDC/EQU-EQU/29737/2017.

CRediT authorship contribution statement

Julio E. Sosa: Formal analysis, Investigation, Visualization, Writing – original draft. **Rui P.P.L. Ribeiro:** Conceptualization, Methodology, Supervision, Writing – review & editing. **Paulo J. Castro:** Formal analysis, Writing – original draft, Writing – review & editing. **José P.B. Mota:** Conceptualization, Funding acquisition, Investigation, Methodology, Project administration, Resources, Supervision, Writing – review & editing. **Ana B. Pereiro:** Conceptualization, Funding acquisition, Methodology, Project administration, Resources, Supervision, Writing – review & editing. **João M.M. Araújo:** Conceptualization, Funding acquisition, Methodology, Project administration, Resources, Supervision, Writing – review & editing.

Declaration of Competing Interest

The authors declare that they have no known competing financial interests or personal relationships that could have appeared to influence the work reported in this paper.

Data availability

Data will be made available on request.

Appendix A. Supplementary material

Supplementary data associated with this article can be found in the online version at doi:10.1016/j.jece.2022.108580.

References

[1] B.S. Akkimaradi, M. Prasad, P. Dutta, K. Srinivasan, Adsorption of 1,1,1,2-tetrafluoroethane on activated charcoal, J. Chem. Eng. Data 46 (2001) 417–422, https://doi.org/10.1021/je000277e.

[2] S. Asensio-Delgado, F. Pardo, G. Zarca, A. Urtiaga, Vapor–liquid equilibria and diffusion coefficients of difluoromethane, 1,1,1,2-tetrafluoroethane, and 2,3,3,3-tetrafluoropropene in low-viscosity ionic liquids, J. Chem. Eng. Data 65 (2020) 4242–4251, https://doi.org/10.1021/acs.jced.0c00224.

[3] S. Asensio-Delgado, F. Pardo, G. Zarca, A. Urtiaga, Absorption separation of fluorinated refrigerant gases with ionic liquids: equilibrium, mass transport, and process design, Sep. Purif. Technol. 276 (2021) 119363, https://doi.org/10.1016/j.seppur.2021.119363.

[4] A.A. Askalany, M. Salem, I.M. Ismail, A.H.H. Ali, M.G. Morsy, Experimental study on adsorption-desorption characteristics of granular activated carbon/R134a pair, Int. J. Refrig 35 (2012) 494–498, https://doi.org/10.1016/j.ijrefrig.2011.04.002.

[5] A.A. Askalany, B.B. Saha, K. Uddin, T. Miyzaki, S. Koyama, K. Srinivasan, I. M. Ismail, Adsorption isotherms and heat of adsorption of difluoromethane on activated carbons, J. Chem. Eng. Data 58 (2013) 2828–2834, https://doi.org/10.1021/je4005678.

[6] A. Askalany, C. Olkis, E. Bramanti, D. Lapshin, L. Calabrese, E. Proverbio, A. Freni, G. Santori, Silica-supported ionic liquids for heat-powered sorption desalination, ACS Appl. Mater. Interfaces 11 (40) (2019) 36497–36505, https://doi.org/10.1021/acsami.9b07602.

[7] M. Attalla, S. Sadek, Experimental investigation of granular activated carbon/R-134a pair for adsorption cooling system applications, J. Power Energy Eng. 2 (2014) 11–20, https://doi.org/10.4236/jpee.2014.22002.

[8] P.J. Castro, A.E. Redondo, J.E. Sosa, M.E. Zakrzewska, A.V.M. Nunes, J.M. M. Araújo, A.B. Pereiro, Absorption of fluorinated greenhouse gases in deep eutectic solvents, Ind. Eng. Chem. Res. 59 (2020) 13246–13259, https://doi.org/10.1021/acs.iecr.0c01893.

[9] L. Dong, D. Zheng, G. Sun, X. Wu, Vapor−liquid equilibrium measurements of difluoromethane + [Emim]OTf, difluoromethane + [Bmim]OTf, difluoroethane + [Emim]OTf, and difluoroethane + [Bmim]OTf systems, J. Chem. Eng. Data 56 (2011) 3663–3668, https://doi.org/10.1021/je2005566.

[10] M.M. Dubinin, The potential theory of adsorption of gases and vapors for adsorbents with energetically nonuniform surfaces, Chem. Rev. 60 (1960) 235–241, https://doi.org/10.1021/cr60204a006.

[11] European Commission, Preparatory Study for a Review of Regulation (EC) No 842/2006 on Certain Fluorinated Greenhouse Gases, 2011.

[12] E. Heath, Amendment to the Montreal Protocol on substances that deplete the ozone layer (Kigali Amendment), Int. Leg. Mater. 56 (2017) 193–205, https://doi.org/10.1017/ilm.2016.2.

[13] C. Hermida-Merino, F. Pardo, G. Zarca, J.M.M. Araújo, A. Urtiaga, M.M. Pineiro, A. B. Pereiro, Integration of stable ionic liquid-based nanofluids into polymer membranes, part I: membrane synthesis and characterization, Nanomaterials 11 (2021) 607–623, https://doi.org/10.3390/nano11030607.

[14] K. Kumar, A. Kumar, Enhanced CO_2 adsorption and separation in ionic-liquid-impregnated mesoporous silica MCM-41: a molecular simulation study, J. Phys. Chem. C 122 (2018) 8216–8227, https://doi.org/10.1021/acs.jpcc.7b11529.

[15] X. Liu, M. He, N. Lv, X. Qi, C. Su, Solubilities of R-161 and R-143a in 1-Hexyl-3-methylimidazolium bis(trifluoromethylsulfonyl)- imide, Fluid Phase Equilib. 388 (2015) 37–42, https://doi.org/10.1016/j.fluid.2014.12.026.

[16] X. Liu, M. He, N. Lv, X. Qi, C. Su, Vapor-liquid equilibrium of three hydrofluorocarbons with [HMIM][Tf_2N], Chem. Eng. Data 60 (2015) 1354–1361, https://doi.org/10.1021/je501069b.

[17] X. Liu, N. Lv, C. Su, M. He, Solubilities of R32, R245fa, R227ea and R236fa in a phosphonium-based ionic liquid, J. Mol. Liq. 218 (2016) 525–530, https://doi.org/10.1016/j.molliq.2016.02.041.

[18] X. Liu, P. Pan, M. He, Vapor-liquid equilibrium and diffusion coefficients of R32 + [HMIM][FEP], R152a + [HMIM][FEP] and R161 + [HMIM][FEP], J. Mol. Liq. 253 (2018) 28–35, https://doi.org/10.1016/j.molliq.2018.01.032.

[19] W.S. Loh, M. Kumja, K.A. Rahman, K.C. Ng, B.B. Saha, S. Koyama, I.I. El-Sharkawy, Adsorption parameter and heat of adsorption of activated carbon/HFC-134a pair, Heat Transf. Eng. 31 (2010) 910–916, https://doi.org/10.1080/01457631003603949.

[20] W.S. Loh, A.B. Ismail, B. Xi, K.C. Ng, W.G. Chun, Adsorption isotherms and isosteric enthalpy of adsorption for assorted refrigerants on activated carbons, J. Chem. Eng. Data 57 (2012) 2766–2773, https://doi.org/10.1021/je3008099.

[21] M. Mohamedali, H. Ibrahim, A. Henni, Imidazolium based ionic liquids confined into mesoporous silica MCM-41 and SBA-15 for carbon dioxide capture, Microporous Mesoporous Mater. 294 (2020), 109916, https://doi.org/10.1016/j.micromeso.2019.109916.

[22] A.R.C. Morais, A.N. Harders, K.R. Baca, G.M. Olsen, B.J. Befort, A.W. Dowling, E. J. Maginn, M.B. Shiflett, Phase equilibria, diffusivities, and equation of state modeling of HFC-32 and HFC-125 in imidazolium-based ionic liquids for the separation of R-410A, Ind. Eng. Chem. Res. 59 (2020) 18222–18235, https://doi.org/10.1021/acs.iecr.0c02820.

[23] A. Mota-Babiloni, P. Makhnatch, R. Khodabandeh, Recent investigations in HFCs substitution with lower GWP synthetic alternatives: focus on energetic performance and environmental impact, Int. J. Refrig. 82 (2017) 288–301, https://doi.org/10.1016/j.ijrefrig.2017.06.026.

[24] R. Motkuri, K. Annapureddy, H.V.R. Vijaykumar, M. Schaef, H.T. Martin, P. F. McGrail, B.P. Dang, L.X. Krishna, R. Thallapally, P.K, Fluorocarbon adsorption in hierarchical porous frameworks, Nat. Commun. 5 (2014) 1–6, https://doi.org/10.1038/ncomms5368.

[25] A.L. Myers, J.M. Prausnitz, Thermodynamics of mixed-gas adsorption, AIChE J. 11 (1965) 121–127, https://doi.org/10.1002/aic.690110125.

[26] F. Pardo, G. Zarca, A. Urtiaga, Separation of refrigerant gas mixtures containing R32, R134a, and R1234yf through poly(ether-block-amide) membranes, ACS Sustain. Chem. Eng. 8 (2020) 2548–2556, https://doi.org/10.1021/acssuschemeng.9b07195.

[27] F. Pardo, S. Gutierrez-Hernandez, C. Hermida-Merino, J.M.M. Araújo, M. M. Pineiro, A.B. Pereiro, G. Zarca, A. Urtiaga, Integration of stable ionic liquid-based nanofluids into polymer membranes. Part II: gas separation properties toward fluorinated greenhouse gases, Nanomaterials 11 (2021) 1–19, https:// doi.org/10.3390/nano11030607.

[28] F. Pardo, G. Zarca, A. Urtiaga, Effect of feed pressure and long-term separation performance of Pebax-ionic liquid membranes for the recovery of difluoromethane (R32) from refrigerant mixture R410A, J. Membr. Sci. 618 (2021), 118744, https://doi.org/10.1016/j.memsci.2020.118744.
[29] F. Pardo, S.V. Gutierrez-Hernandez, G. Zarca, A. Urtiaga, Toward the recycling of low-GWP hydrofluorocarbon/hydrofluoroolefin refrigerant mixtures using composite ionic liquid-polymer membranes. ACS Sustain, Chem. Eng. 9 (20) (2021) 7012–7021, https://doi.org/10.1021/acssuschemeng.1c00668.
[30] A.B. Pereiro, J.M.M. Araújo, S. Martinho, F. Alves, A. Matias, C.M.M. Duarte, L.P. N. Rebelo, I.M. Marrucho, Fluorinated ionic liquids: properties and applications, ACS Sustain. Chem. Eng. 1 (2013) 427–439, https://doi.org/10.1021/sc300163n.
[31] A.B. Pereiro, L.C. Tomé, S. Martinho, L.P.N. Rebelo, I.M. Marrucho, Gas permeation properties of fluorinated ionic liquids, Ind. Eng. Chem. Res. 52 (2013) 4994–5001, https://doi.org/10.1021/ie4002469.
[32] A.B. Pereiro, M.J. Pastoriza-Gallego, K. Shimizu, I.M. Marrucho, J.N.C. Lopes, M. M. Piñeiro, L.P.N. Rebelo, On the formation of a third, nanostructured domain in ionic liquids, J. Phys. Chem. B 117 (2013) 26–33, https://doi.org/10.1021/jp402300c.
[33] J.M. Prausnitz, R.N. Lichtenthaler, E.G. Azevedo. Molecular Thermodynamics of Fluid-phase Equilibria, 3rd ed., Prentice-HallPTR, UpperSaddle River. NJ, 1999 https://doi.org/10.1002/cjce.5450780222.
[34] W. Ren, A.M. Scurto, Phase equilibria of imidazolium ionic liquids and the refrigerant gas, 1,1,1,2-tetrafluoroethane (R-134a, Fluid Phase Equilib. 286 (2009) 1–7, https://doi.org/10.1016/j.fluid.2009.07.007.
[35] G.E. Romanos, P.S. Schulz, M. Bahlmann, P. Wasserscheid, A. Sapalidis, F. K. Katsaros, C.P. Athanasekou, K. Beltsios, N.K. Kanellopoulos, CO_2 capture by novel supported ionic liquid phase systems consisting of silica nanoparticles encapsulating amine-functionalized ionic liquids, J. Phys. Chem. C 118 (2014) 24437–24451, https://doi.org/10.1021/jp5062946.
[36] B.B. Saha, K. Habib, I.I. El-Sharkawy, S. Koyama, Adsorption characteristics and heat of adsorption measurements of R-134a on activated carbon, Int. J. Refrig. 32 (2009) 1563–1569, https://doi.org/10.1016/j.ijrefrig.2009.03.010.
[37] B.B. Saha, I.I. El-Sharkawy, R. Thorpe, R.E. Critoph, Accurate adsorption isotherms of R134a onto activated carbons for cooling and freezing applications, Int. J. Refrig. 35 (2012) 499–505, https://doi.org/10.1016/j.ijrefrig.2011.05.002.
[38] M. Sattaria, A. Kamaria, H. Hashemia, A.H. Mohammadib, D. Ramjugernath, A group contribution model for prediction of the viscosity with temperature dependency for fluorine-containing ionic liquids, J. Fluor. Chem. 186 (2016) 19–27, https://doi.org/10.1016/j.jfluchem.2016.04.001.
[39] S. Savitz, S.M. Tieri, R.J. Gorte, C.P. Grey, R. Huber, A.L. Myers, D.R. Corbin, F. R. Siperstein, Adsorption of hydrofluorocarbons HFC-134 and HFC-134A on X and Y zeolites: effect of ion-exchange on selectivity and heat of adsorption, J. Phys. Chem. B 103 (1999) 8283–8289, https://doi.org/10.1021/jp990560o.
[40] M.B. Shiflett, M.A. Harmer, C.P. Junk, A. Yokozeki, Solubility and diffusivity of difluoromethane in room-temperature ionic liquids, Chem. Eng. Data 51 (2006) 483–495, https://doi.org/10.1021/je050386z.
[41] M.B. Shiflett, A. Yokozeki, Absorption Cycle Utilizing Ionic Liquid as Working Fluid, EP 1846535A1, 2005.
[42] M.B. Shiflett, A. Yokozeki, Solubility and diffusivity of hydrofluorocarbons in room-temperature ionic liquids, AIChE J. 52 (2006) 1205–1219, https://doi.org/10.1002/aic.10685.
[43] M.B. Shiflett, A. Yokozeki, Solubility differences of halocarbon isomers in ionic liquid [emim][Tf_2N], J. Chem. Eng. Data 52 (2007) 2007–2015, https://doi.org/10.1021/je700295e.
[44] M.B. Shiflett, A. Yokozeki, Binary vapor-liquid and vapor-liquid-liquid equilibria of hydrofluorocarbons (HFC-125 and HFC- 143a) and hydrofluoroethers (HFE-125 and HFE-143a) with ionic liquid [emim][Tf_2N], J. Chem. Eng. Data 53 (2008) 492–497, https://doi.org/10.1021/je700588d.
[45] R. Sips, On the structure of a catalyst surface, J. Chem. Phys. 16 (1948) 490–495, https://doi.org/10.1063/1.1746922.
[46] J.E. Sosa, R.P.P.L. Ribeiro, P.J. Castro, J.P.B. Mota, J.M.M. Araújo, A.B. Pereiro, Absorption of fluorinated greenhouse gases using fluorinated ionic liquids, Ind. Eng. Chem. Res. 58 (2019) 20769–20778, https://doi.org/10.1021/acs.iecr.9b04648.
[47] J.E. Sosa, C. Malheiro, R.P.P.L. Ribeiro, P.J. Castro, M.M. Piñeiro, J.M.M. Araújo, F. Plantier, J.P.B. Mota, A.B. Pereiro, Adsorption of fluorinated greenhouse gases on activated carbons: evaluation of their potential for gas separation, J. Chem. Technol. Biotechnol. 95 (2020) 1892–1905, https://doi.org/10.1002/jctb.6371.
[48] J.E. Sosa, R. Santiago, A.E. Redondo, J. Avila, L.F. Lepre, M.C. Gomes, J. Palomar, A.B. Pereiro, J.M.M. Araújo, Design of ionic liquids for fluorinated gas absorption: COSMO-RS selection and solubility experiments, Environ. Sci. Technol. 56 (2022) 5898–5909, https://doi.org/10.1021/acs.est.2c00051.
[49] Q. Su, Y. Qi, X. Yao, W. Cheng, L. Dong, S. Chen, S. Zhang, Ionic liquids tailored and confined by one-step assembly with mesoporous silica for boosting the catalytic conversion of CO_2 into cyclic carbonates, Green Chem. 20 (2018) 3232–3241, https://doi.org/10.1039/C8GC01038B.
[50] United Nations, Handbook for the Montreal Protocol on Substances that Deplete the Ozone Layer, ninth ed., 2012.
[51] N.S.M. Vieira, J.C. Bastos, L.P.N. Rebelo, A. Matias, J.M.M. Araújo, A.B. Pereiro, Human cytotoxicity and octanol/water partition coefficients of fluorinated ionic liquids, Chemosphere 216 (2019) 576–586, https://doi.org/10.1016/j.chemosphere.2018.10.159.
[52] N.S.M. Vieira, S. Stolte, J.M.M. Araújo, L.P.N. Rebelo, A.B. Pereiro, M. Markiewicz, Acute aquatic toxicity and biodegradability of fluorinated ionic liquids, ACS Sustain. Chem. Eng. 7 (2019) 3733–3741, https://doi.org/10.1021/acssuschemeng.8b03653.
[53] D.K.J.A. Wanigarathna, J. Gao, T. Takanami, Q. Zhang, B. Liu, Adsorption separation of R-22, R-32 and R-125 fluorocarbons using 4A molecular sieve zeolite, Chemistry Select 1 (2016) 3718–3722, https://doi.org/10.1002/slct.201600689.
[54] D.K.J.A. Wanigarathna, J. Gao, B. Liu, Metal organic frameworks for adsorption-based separation of fluorocompounds: a review, Mater. Adv. 1 (2020) 310, https://doi.org/10.1039/d0ma00083c.
[55] A.D. Yancey, S.J. Terian, B.J. Shaw, T.M. Bish, D.R. Corbin, M.B. Shiflett, A review of fluorocarbon sorption on porous materials, Microporous Mesoporous Mater. 331 (2022), 111654, https://doi.org/10.1016/j.micromeso.2021.111654.